

## Age affects the strain-rate dependence of mechanical properties of kelp tissues

Nicholas P. Burnett<sup>1,2,3</sup>  and M.A.R. Koehl<sup>1</sup>

Manuscript received 6 November 2020; revision accepted 7 January 2021.

<sup>1</sup> Department of Integrative Biology, University of California, Berkeley, CA 94720, USA

<sup>2</sup> Present address: Department of Neurobiology, Physiology, and Behavior, University of California, Davis, CA 95616, USA

<sup>3</sup> Author for correspondence (e-mail: burnettnp@gmail.com)

**Citation:** Burnett, N. P. and M. A. R. Koehl. 2021. Age affects the strain-rate dependence of mechanical properties of kelp tissues. *American Journal of Botany* 108(5): 1–8.

doi:10.1002/ajb2.1662

**PREMISE:** The resistance of macroalgae to hydrodynamic forces imposed by ambient water motion depends in part on the mechanical properties of their tissues. In wave-swept habitats, tissues are stretched (strained) at different rates as hydrodynamic forces change. Previous studies of mechanical properties of macroalgal tissues have used either a single strain rate or a small range of strain rates. Therefore, our knowledge of the mechanical properties of macroalgae is limited to a narrow fraction of the strain rates that can occur in nature. In addition, although mechanical properties of macroalgal tissues change with age, the effect of age on the strain-rate dependence of their mechanical behavior has not been documented.

**METHODS:** Using the kelp *Egregia menziesii*, we measured how high strain rate (simulating wave impingement) and low strain rate (simulating wave surge) affected mechanical properties of frond tissues of various ages.

**RESULTS:** Stiffness of tissues of all ages increased with strain rate, whereas extensibility was unaffected. Strength and toughness increased with strain rate for young tissue but were unaffected by strain rate for old tissue.

**CONCLUSIONS:** Young tissue is weaker than old tissue and, therefore, the most susceptible to breakage from hydrodynamic forces. The increased strength of young tissue at high strain rates can help the frond resist breaking when pulled rapidly during wave impingement, when hydrodynamic forces are largest. Because breakage of young tissue can remove a frond's meristem and negatively impact the survival of the whole kelp, strain-rate dependence of the young tissue's strength can enhance kelp's survival.

**KEY WORDS** deformation; Laminariales; macrophytes; material properties; phycology; rheology.

Macroalgae on wave- and current-swept shores are subjected throughout their lives to hydrodynamic forces imposed by ambient water motion (e.g., Koehl and Wainwright, 1977; Denny, 1988; Carrington, 1990; Kitzes and Denny, 2005; Gaylord et al., 2008). The size, shape, and flexibility of a macroalga affect the magnitude of the hydrodynamic forces it experiences in ambient water flow (e.g., Koehl, 1985, 1999; Denny, 1988; Carrington, 1990), and the geometry of the thallus determines the magnitude of the stresses in the tissues when exposed to those forces (e.g., Johnson and Koehl, 1994; Koehl 1999). The mechanical properties of the tissues ("material properties") of macroalgae influence how they deform and whether they are damaged or break when exposed to the stresses caused by hydrodynamic forces (e.g., Delf, 1932; Koehl and Wainwright, 1977; Koehl, 1985, 1999; Denny, 1988; Carrington, 1990; Johnson and Koehl, 1994; Denny et al., 2013; Starko et al., 2018). For example,

the stretching or bending of a macroalga in flowing water depends in part on the stiffness (elastic modulus) of its tissues. Whether or not hydrodynamic forces rip off parts of a macroalga depends on the strength (force per cross-sectional area required to break a material) and toughness (work per volume required to break a material) of its tissues. Macroalgal tissues can be tough either by being strong or by being very extensible (stretching a great deal before breaking). Quantifying these material properties can reveal how macroalgae withstand different magnitudes and temporal regimes of hydrodynamic forces encountered in their natural habitats (e.g., Koehl, 1999).

Hydrodynamic forces on macroalgae and the resulting rates at which their tissues are strained are constantly changing. Macroalgae, which move back-and-forth in wave-driven flow (Koehl, 1986, 1999) and flutter in turbulent unidirectional flow (Koehl and

Alberte, 1988), are exposed to changes in ambient water motion that occur over a range of time scales, from the impingement and surge portions of a single wave hitting the shore (Gaylord, 1999; Gaylord et al., 2003; Jensen and Denny, 2015) to the changes in flow that occur during tidal cycles (e.g., Koehl and Alberte, 1988) and between different seasons (Burnett and Koehl, 2020). Although macroalgae are exposed to a wide range of strain rates from fluctuating ambient water flow, the effects of different ecologically relevant strain rates on their material properties, and thus their performance in flow, is poorly understood.

Many biomaterials are viscoelastic, so their material properties depend on the rate at which they are strained (e.g., Alexander, 1964; Denny and Gosline, 1980; Mason and Weitz, 1995; Zhou et al., 2009; Sahni et al., 2010; Hayot et al., 2012; Meyers and Chen, 2014). For example, the body-wall tissue of sea anemones is stiff when exposed to high strain rates mimicking those they experience in waves (enabling them to remain upright to capture prey in waves) but is very compliant when exposed to the low strain rates experienced in tidal currents (enabling them to passively reorient in the ambient flow) (Koehl, 1977). Similarly, the stiffness of the

byssal threads attaching mussels to the substratum increases with strain rate when cyclically stretched, as they are when mussels are battered by waves (Carrington and Gosline, 2004). Other mechanical behaviors of viscoelastic materials include hysteresis during cyclic loading (i.e., the material stretches when loaded but does not immediately return to its original length when unloaded) and creep (i.e., the material deforms over time when a static load is applied) (Koehl, 1977; Vincent, 2012). Several species of macroalgae show time-dependent material properties in cyclic loading or creep tests (e.g., Johnson and Koehl, 1994; Hale, 2001; Harder et al., 2006; Denny et al., 2013), but little is known about how different strain rates affect the deformation and breakage of macroalgal tissues in nature. Although many studies of the material properties of macroalgae do not report the strain rates used in mechanical tests, strain rates that have been published for some studies of macroalgae are summarized in Table 1. Only a few studies tested multiple strain rates, and of those only one study provided a quantitative justification that the strain rates used mimicked those experienced by macroalgal tissues in natural flow (Burnett and Koehl, 2018). Overall, the strain-rate

**TABLE 1.** Examples of strain rates used to measure material properties of macroalgae in pull-to-break tests. Notes of the measured structures are based on the descriptions in the referenced literature (Ref.). \* Studies that compared material properties by tissue age. \*\* Studies that controlled for tissue age, e.g., by measuring tissue at a specific location on the thallus.

| Order        | Species name                         | Structure measured | Strain rate (strain/s)                         | Effect of strain rate?   | Ref. |
|--------------|--------------------------------------|--------------------|--|--|------|
| Fucales      | <i>Ascophyllum nodosum</i>           | Frond axis         | 1  |  | 1**  |
|              | <i>Durvillaea antarctica</i>         | Stipe              | $1.67 \times 10^{-3}$ to $6.67 \times 10^{-3}$ | Not reported   | 2    |
|              | <i>Durvillaea willana</i>            | Stipe              | $1.67 \times 10^{-3}$ to $6.67 \times 10^{-3}$ | Not reported   | 2    |
|              | <i>Fucus distichus</i>               | Blade              | 0.05   |  | 3    |
|              | <i>Pelvetiopsis californica</i>      | Blade              | 0.05   |  | 3    |
|              | <i>Pelvetiopsis limitata</i>         | Branch axis        | $2.50 \times 10^{-2}$ to $1.81 \times 10^{-2}$ | No effect on <i>E</i>  | 4    |
|              | <i>Silvetia compressa</i>            | Blade              | 0.05   |  | 3    |
|              | <i>Turbinaria ornata</i>             | Stipe              | $1.6 \times 10^{-2}$                           |  | 5    |
|              | <i>Alaria marginata</i>              | Blade, stipe       | 0.05   |  | 3    |
|              | <i>Dictyoneurum</i> sp.              | Blade              | 0.05   |  | 3    |
| Laminariales | <i>Egregia menziesii</i>             | Rachis             | $3.33 \times 10^{-3}$ to $1.58 \times 10^{-2}$ | No effect on <i>E</i>  | 6**  |
|              |                                      | Rachis             | $3.33 \times 10^{-3}$                          |  | 7*   |
|              |                                      | Rachis             | 0.05   |  | 3    |
|              | <i>Laminaria digitata</i>            | Stipe              | $1.67 \times 10^{-3}$ to $6.67 \times 10^{-3}$ | Not reported   | 2    |
|              |                                      | Blade, stipe       | $1.17 \times 10^{-1}$                          |  | 8**  |
|              | <i>Laminaria hyperborea</i>          | Stipe              | $1.67 \times 10^{-3}$ to $6.67 \times 10^{-3}$ | Not reported   | 2    |
|              |                                      | Blade, stipe       | $1.17 \times 10^{-1}$                          |  | 8**  |
|              | <i>Laminaria setchellii</i>          | Blade              | 0.05   |  | 3    |
|              | <i>Macrocystis pyrifera</i>          | Blade, stipe       | 0.05   |  | 3    |
|              | <i>Nereocystis luetkeana</i>         | Stipe              | 0.05   |  | 3    |
| Corallinales |                                      | Stipe              | $2.5 \times 10^{-2}$ to $8.4 \times 10^{-2}$   | No effect on $\sigma_{\max}$ , $\lambda_{\max}$ , <i>E</i> , or <i>W/V</i> | 9**  |
|              | <i>Postelsia palmaeformis</i>        | Blade, stipe       | 0.05   |  | 3    |
|              | <i>Pterygophora californica</i>      | Blade              | $3.33 \times 10^{-2}$                          |  | 10** |
|              | <i>Saccharina latissima</i>          |                    | $5.56 \times 10^{-3}$                          |  | 11   |
| Gigartinales | <i>Calliarthron cheilosporioides</i> | Frond, geniculum   | 0.05   |  | 3    |
|              |                                      | Frond              | 38 to 61                                       | Not reported   | 12   |
|              | <i>Chondracanthus exasperatus</i>    | Blade              | $3.0 \times 10^{-3}$ to $3.0 \times 10^{-2}$   | No effect on $\sigma_{\max}$ , $\lambda_{\max}$ , <i>E</i> , or <i>W/V</i> | 13   |
|              | <i>Chondracanthus harveyanus</i>     | Blade              | 0.05   |  | 3    |
|              | <i>Endocladia muricata</i>           | Stipe              | 0.05   |  | 3    |
|              | <i>Mazzaella flaccida</i>            | Blade              | 0.05   |  | 3    |
|              |                                      | Blade              | 0.19   |  | 14   |
|              | <i>Mazzaella splendens</i>           | Blade              | 0.19   |  | 14   |

References: <sup>1</sup>Lowell et al., 1991; <sup>2</sup>Harder et al., 2006; <sup>3</sup>Hale, 2001; <sup>4</sup>Wolcott, 2007; <sup>5</sup>Stewart, 2006; <sup>6</sup>Burnett and Koehl, 2018; <sup>7</sup>Burnett and Koehl, 2019; <sup>8</sup>Henry, 2018; <sup>9</sup>Johnson and Koehl, 1994; <sup>10</sup>Biedka et al., 1987; <sup>11</sup>Vettori and Nikora, 2017; <sup>12</sup>Denny et al., 2013; <sup>13</sup>Koehl, 2000; <sup>14</sup>Mach, 2009.

dependence of tissue mechanical properties of macroalgae is poorly understood in the context of the range of strain rates encountered in their natural habitats.

The mechanical properties of biological tissues can change with age (e.g., Meinzer et al., 2011; Derby and Akhtar, 2015; Morgan et al., 2018), and a few studies have documented age-related differences in the material properties of macroalgal tissues (Armstrong, 1988; Johnson and Koehl, 1994; Krumhansl et al., 2015; Burnett and Koehl, 2019). Macroalgae and plants are composed of tissues of different ages that function together to produce the mechanical behavior of the whole organism (e.g., Meinzer et al., 2011; Krumhansl et al., 2015). However, understanding the mechanical responses of these organisms when exposed to ecologically relevant loading patterns requires knowledge of whether tissue age affects the strain-rate dependence of mechanical properties.

We used the intertidal kelp *Egregia menziesii* to test whether strain rate within the range experienced in wave-swept habitats affects the material properties of macroalgal tissues of different ages. *Egregia menziesii* is a dominant intertidal kelp (Laminariales) on wave-exposed rocky shores along the west coast of North America (Abbott and Hollenberg, 1976). An individual thallus has a single holdfast anchored to the substratum and numerous strap-like fronds (Abbott and Hollenberg, 1976). Each frond has a rachis that can grow to several meters in length and that bears lateral blades and gas-filled pneumatocysts along its edges. During an individual's lifetime, which can be multiple years, fronds are frequently broken and replaced by new fronds, thus the morphology of the thallus is not necessarily indicative of the individual kelp's age (Black, 1974; Demes et al., 2013; Burnett and Koehl, 2020). Most of a frond's growth occurs as extension at its distal intercalary meristem (Fig. 1), so rachis tissue near the holdfast is older than rachis tissue near the intercalary meristem (Black, 1974). Although we have shown that the material properties of the rachis of *E. menziesii*, measured at a single strain rate, change along the length of the rachis (i.e., change with age) (Burnett and Koehl, 2019), the effect of tissue age on the strain-rate dependence of those properties has not been studied.

The current study goes beyond our earlier work to pursue two objectives: (1) to test whether strain rate affects the material properties of the rachis of *E. menziesii* and (2) to determine whether the effect of strain rate on material properties depends on the age of the tissue. Another goal of our study was to determine the effects of strain rates that represent a much wider range of ecologically relevant strain rates than have been examined previously for kelp or other macroalgae (Table 1). The specific questions we addressed were: (1) Are there differences in material properties of rachis tissue subjected

to strain rates that mimic those of the impingement versus surge stages of a wave hitting the shore? (2) Are the strain-rate dependences of rachis material properties affected by tissue age?

## MATERIALS AND METHODS

### Field site and collection

In May 2017, fronds of *Egregia menziesii* were collected from two sites in northern California: 20 fronds were collected from Miwok Beach ( $38^{\circ}21'25''N$ ,  $123^{\circ}4'2''W$ ) near Bodega, California, and 12 fronds were collected from McClures Beach ( $38^{\circ}11'3''N$ ,  $122^{\circ}58'2''W$ ) from the Point Reyes National Seashore. During this month, the significant wave heights (average of the 33% largest waves) measured hourly at a buoy near both sites were 2.1 m (mean; minimum = 0.8 m; maximum = 5.1 m; Buoy 46013, www.ndbc.noaa.gov). In a concurrent study, material properties of *E. menziesii* were compared between sites and found to be similar (Burnett and Koehl, 2019). At each site, fronds were collected by walking along a transect parallel to the shoreline and haphazardly removing a frond from every third *E. menziesii* encountered. Fronds were only collected if they were  $\geq 40$  cm long, unwounded (i.e., no damage from herbivores), and had their intercalary meristem (Burnett and Koehl, 2019). Fronds were stored in a cooler between  $11^{\circ}$  and  $15^{\circ}C$  with just the water that was trapped on the fronds and transported to UC Berkeley. Material properties were measured within 12 h.

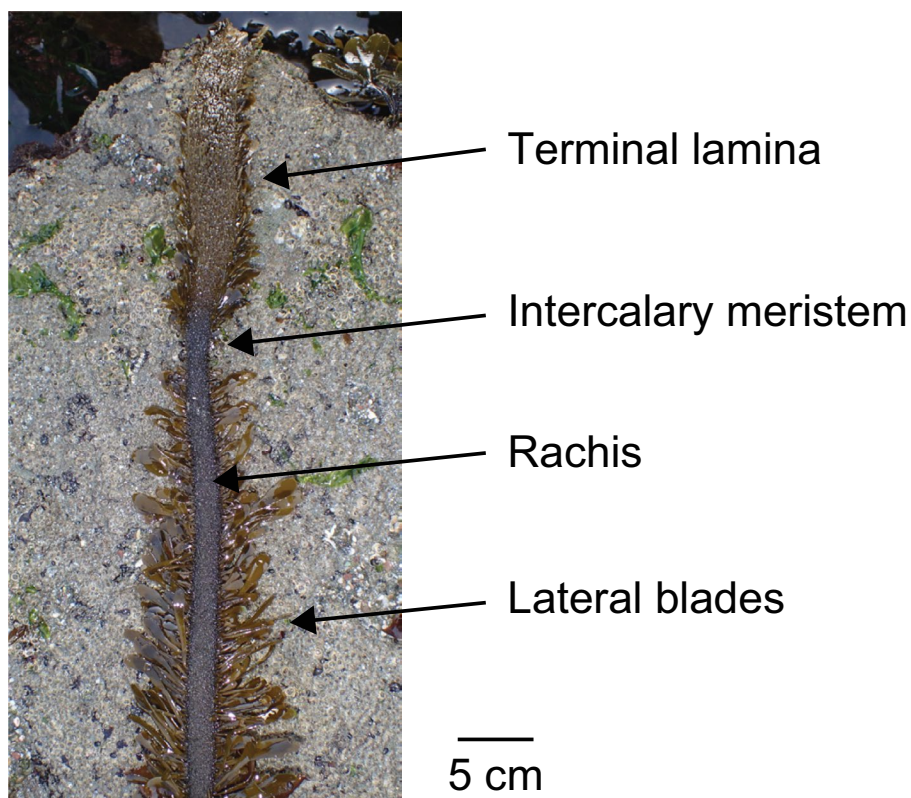


**FIGURE 1.** Anatomy of a frond of *Egregia menziesii*. The terminal lamina, intercalary meristem, rachis, and lateral blades are labeled. Tissue near the intercalary meristem is younger than tissue far from the meristem.

## Measuring material properties

We measured the material properties of rachis tissue by conducting tensile stress-strain tests (as detailed by Koehl and Wainwright, 1985). A Model 5544 Instron materials-testing machine (Instron, Norwood, MA, USA) was used to pull on a section of rachis at a defined strain rate until it broke, while simultaneously measuring the specimen extension and the force with which it resisted the deformation. We define “strain rate” as the change in length per time of a sample divided by the sample’s original length. We use engineering stress-strain definitions, which are common in studies of macroalgal mechanics, where “engineering stress” is defined as the force acting on a sample divided by the sample’s original cross-sectional area, and “engineering strain” is the total change in the sample’s length divided by the sample’s original length. In studies of macroalgal mechanics, engineering strain is often reported as extension ratio, which is the total length of the sample divided by the sample’s original length (i.e., engineering strain + 1), and we follow this convention here. We also consider the true stress-strain definitions, which are appropriate for materials that are highly deformable, including macroalgal tissue: “True stress” is the instantaneous force acting on a sample divided by the sample’s instantaneous cross-sectional area, and “true strain” is the instantaneous extension of the sample relative to the previous instantaneous length, which is calculated as  $\ln(1 + \text{engineering strain})$  (Vincent, 2012). We calculated the instantaneous cross-sectional area of the sample by dividing the sample’s volume, which remains constant, by its instantaneous length. A variety of material properties can be calculated from the resulting stress-strain curve, whether represented as engineering stress-strain or true stress-strain (Fig. 2).

We measured material properties of *E. menziesii* rachis tissue of different ages. For each frond, we cut sections (10 cm long) of the intact rachis at specific distances from the intercalary meristem, where distance from meristem indicates tissue age (Burnett and Koehl, 2019): 0 to 10 cm, 20 to 30 cm, 40 to 50 cm, and 60 to 70 cm. For simplicity, we will hereafter refer to these rachis regions by the mean distance of each sample from the intercalary meristem (i.e., 5, 25, 45,

and 65, respectively). Some fronds were not long enough to provide tissue at each region. The ends of each sample were wrapped with pieces of paper towel that were affixed to the specimen by cyanoacrylate glue to prevent slipping in the grips of the Instron. Each sample was then secured in the grips of the Instron and strain was applied at a fixed rate (see below) until the sample failed. The force with which the sample resisted the strain was measured at 10 Hz to the nearest 0.1 N, and the extension of the sample was based on the distance between the Instron’s clamps. The cross section of the sample next to the break location was then photographed, and its area ( $A$ ) was measured using ImageJ software v1.52g (U.S. National Institutes of Health, Bethesda, MD, USA).

We used the measurements of force ( $F$ ) and change in sample length  $\Delta L$ , along with the sample’s cross-sectional area ( $A$ ) and original length ( $L_0$ ), to construct an engineering stress-strain curve and true stress-strain curve for each sample (Fig. 2). We then calculated four pairs of material properties for each sample, with one set based on engineering stress-strain curves and the other set based on the true stress-strain curves: (1) Tensile strength,  $\sigma_{\max}$ , is the stress ( $F/A$ ) at which the sample broke; (2) extensibility,  $\lambda_{\max}$ , is the strain at which the sample broke; (3) elastic modulus,  $E$ , is the slope of the initial linear portion of the stress-strain curve between strains 0.0 and 0.1; (4) yield stress,  $\sigma_{yield}$ , is the stress at which the sample exhibited plastic deformation after it was extended beyond the range of its elastic behavior. Yield stress was identified by fitting a cubic spline regression model to the stress-strain curve and finding the stress at which the rate of change in stress per change in strain was lowest (i.e., where the sample suddenly started deforming without a proportional increase in stress). We also calculated (5) work per volume to fracture,  $W/V$ , which is the mechanical work to fracture the sample normalized by the sample’s volume ( $AL_0$ ), as the total area under the stress-strain curve (i.e., it is independent of whether the curve is presented as engineering vs. true stress-strain). Often,  $W/V$  is referred to as “toughness”.

## Strain rates

Intertidal kelp like *E. menziesii* that live on wave-swept shores encounter a wide range of water flow conditions that vary with tide and season. For this study, we focused on two strain rates that were chosen to represent strain rates encountered by *E. menziesii* exposed to breaking waves that typically occur in late spring and summer (Burnett and Koehl, 2019): a high strain rate that could occur during wave impingement and a low strain rate that could occur during wave surge. Each frond was randomly assigned a strain rate, and all samples from that frond were measured at the same strain rate. In situ measurements of hydrodynamic forces on whole *E. menziesii* showed that loads during the surge portion of waves can increase at rates of approximately 10 N/s (Gaylord et al., 2008). From preliminary stress-strain measurements of *E. menziesii* rachis tissue, we found that a loading rate of 10 N/s corresponds to a strain rate of approximately  $3.33 \times 10^{-3}/\text{s}$ . In situ measurements of water accelerations during complete wave cycles showed that water accelerates on the order of  $100 \text{ m/s}^2$  during wave impingement and on the order of  $1 \text{ m/s}^2$  during wave surge (Gaylord, 1999). We estimated that the water accelerations during impingement that are 100-fold higher than during wave surge could produce loading and strain rates in *E. menziesii* that are 100 times greater than the rates experienced during wave surge. Therefore, to simulate strain that could occur during wave impingement, we used a strain rate of

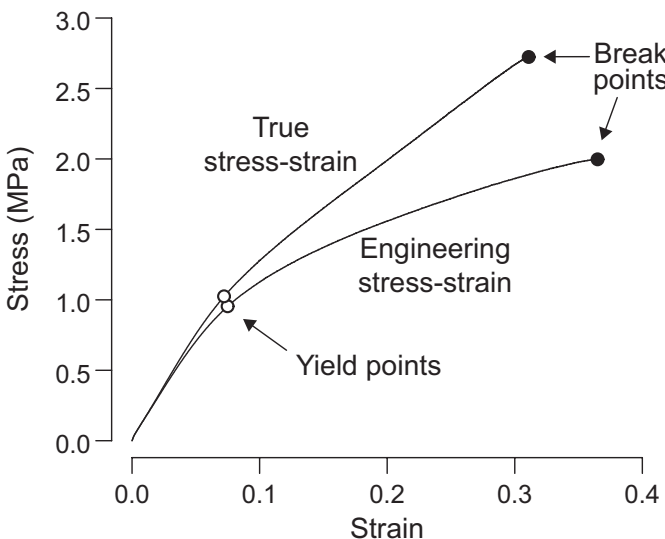


**FIGURE 2.** Comparison of true and engineering stress-strain curves constructed from the same pull-to-break test on rachis tissue of *Egregia menziesii*. For reference, the break points (filled circles) and yield points (open circles) are shown for each curve.

$3.33 \times 10^{-1}/\text{s}$  during stress-strain tests on *E. menziesii* rachis tissue. It is important to note that these two strain rates,  $3.33 \times 10^{-3}/\text{s}$  and  $3.33 \times 10^{-1}/\text{s}$ , are not the only strain rates that may occur during wave surge and wave impingement, respectively, because waves are highly variable across space and time (O'Donnell and Denny, 2008), and many factors influence the specific strain rates that occur in different regions of the kelp's tissues (e.g., the kelp's position in the water, the length of the kelp) (Koehl, 1986, 1999). Instead, these two strain rates represent a range of strain rates that could occur as a wave passes over the kelp, but which has not been examined for its effects on the kelp's material properties.

### Statistical analyses

Each material property was compared between the low and high strain rates using Student's *t*-test with a critical *P*-value of 0.05. Separate analyses were done for each tissue region (i.e., distance from the intercalary meristem) because material properties are known to change along the length of the rachis (Burnett and Koehl, 2019). All analyses were done in the R environment (R Core Team, 2020).

### RESULTS

Strain rate affected certain mechanical properties of the rachis tissue of *Egregia menziesii*, and effects of strain rate were independent of whether material properties were calculated from engineering stress-strain curves or true stress-strain curves (Fig. 3). The elastic modulus (*E*) of tissues of all ages (i.e., all distances from the intercalary meristem) was greater at the high strain rate of wave impingement than at the lower strain rate of wave surge (engineering:  $t \geq 3.10$ ,  $\text{df} \geq 15.94$ ,  $P < 0.005$ ; true:  $t \geq 3.07$ ,  $\text{df} \geq 15.93$ ,  $P \leq 0.005$ ). In contrast, the tensile strength ( $\sigma_{\max}$ ) of rachis tissue was greater at the high strain rate only for young tissue (i.e., 5, 25, 45 cm from the meristem) (engineering:  $t \geq 2.99$ ,  $\text{df} \geq 22.69$ ,  $P \leq 0.006$ ; true:  $t \geq 2.74$ ,  $\text{df} \geq 19.10$ ,  $P < 0.011$ ) but not for older tissue 65 cm from the meristem (engineering:  $t = 1.34$ ,  $\text{df} = 14.1$ ,

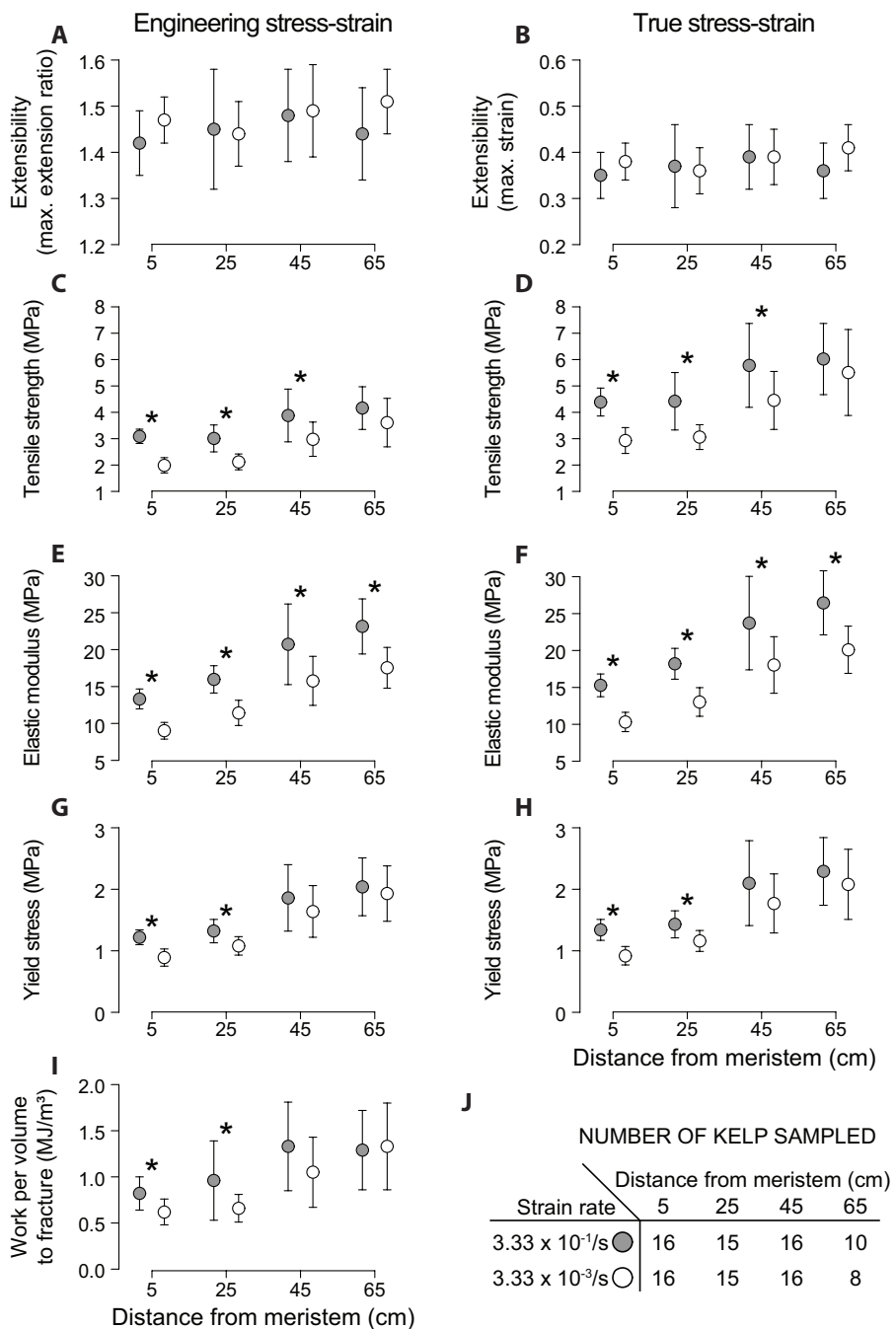


**FIGURE 3.** Material properties of *Egregia menziesii* rachis tissue measured at two strain rates. Material properties are calculated based on both engineering stress-strain curves (A, C, E, G) and true stress-strain curves (B, D, F, H), with equivalent properties plotted on the same row. Extensibility (A, B), tensile strength (C, D), elastic modulus (E, F), yield stress (G, H), and work per volume to fracture (I) are plotted as a function of the tissue's distance from the intercalary meristem, which correlates with the tissue's age (Burnett and Koehl, 2019). Gray symbols show the mean for tissues pulled at the high strain rate,  $3.33 \times 10^{-1}/\text{s}$  (corresponding to the impingement stage of a wave); white symbols show the mean for tissues pulled at the low strain rate,  $3.33 \times 10^{-3}/\text{s}$  (corresponding to the surge stage of a wave). Error bars show one standard deviation; asterisks show tissue regions where strain rate had a significant effect on the material property (Student's *t*-test,  $P < 0.05$  for significance). (J) Sample sizes (number of kelp) for each strain rate and tissue region.

$P = 0.201$ ; true:  $t = 0.71$ ,  $df = 13.59$ ,  $P = 0.491$ ). Yield stress ( $\sigma_{yield}$ ) of rachis tissue was greater at the high strain rate for younger tissue 5 and 25 cm from the meristem (engineering:  $t \geq 3.84$ ,  $df \geq 26.84$ ,  $P < 0.005$ ; true:  $t \geq 3.77$ ,  $df \geq 2.28$ ,  $P < 0.005$ ) but not for older tissue 45 and 65 cm from the meristem (engineering:  $t \leq 1.31$ ,  $df \leq 15.34$ ,  $P \geq 0.202$ ; true:  $t \leq 0.81$ ,  $df \leq 14.87$ ,  $P \geq 0.130$ ). Similarly, toughness (work per volume to fracture,  $W/V$ ) was greater at the high strain rate than at the low strain rate for the younger tissue 5 and 25 cm from the meristem ( $t \geq 2.57$ ,  $df \geq 17.12$ ,  $P \leq 0.020$ ), while the  $W/V$  of older tissue (i.e., 45 and 65 cm from the intercalary meristem) was unaffected by strain rate ( $t \leq 1.85$ ,  $df \leq 28.55$ ,  $P \geq 0.074$ ). Thus, all the rachis tissue was stiffer at the high strain rate of wave impingement than at the low strain rate of wave surge, but only the young tissue was more resistant to breaking and yielding at the high strain rate than at the low strain rate.

Only one material property was independent of strain rate in rachis tissue of all ages (Fig. 3). Each tissue region showed no effect of strain rate on extensibility ( $\lambda_{max}$ ) (engineering:  $t \leq 2.00$ ,  $df \leq 29.92$ ,  $P \geq 0.055$ ; true:  $t \leq 2.02$ ,  $df \leq 29.96$ ,  $P \geq 0.054$ ).

## DISCUSSION

To survive in wave-swept habitats, fronds of *Egregia menziesii* must withstand the hydrodynamic forces from ambient water motion. We found that the age of rachis tissue affects whether high strain rate reduces breakability. Specifically, we found that young tissue (near the meristem) of *E. menziesii* fronds increased its tensile strength ( $\sigma_{max}$ ), resistance to plastic deformation ( $\sigma_{yield}$ ), and toughness (i.e., work per volume to fracture,  $W/V$ ) under high strain rate (Fig. 3C, G, I). This pattern can affect the survival of fronds because the highest strain rates and largest hydrodynamic forces can occur during the impingement portion of a wave (Gaylord, 1999; Gaylord et al., 2008; but see Jensen and Denny, 2015), and the young tissue is the weakest point on a frond (i.e., has the lowest  $\sigma_{max}$ ) (Burnett and Koehl, 2019). The strain-rate dependence of  $\sigma_{max}$  allows young tissue to have nearly the same  $\sigma_{max}$  as old tissue when the frond is strained rapidly by hydrodynamic forces (Fig. 3A). The strain-rate dependence of  $\sigma_{yield}$  and  $W/V$  in young tissue also allows the young tissue to have more resistance to plastic deformation and be tougher (i.e., requiring more mechanical work to break), respectively, when strained quickly than when strained slowly. The spatial pattern of  $\sigma_{max}$ ,  $\sigma_{yield}$ , and  $W/V$  likely exists because material properties depend on the tissue's cellular structure, and features such as cell wall thickness increase with age (Starko et al., 2018). Therefore, the strain rate-dependence of  $\sigma_{max}$ ,  $\sigma_{yield}$ , and  $W/V$  allows young tissue to have a similar mechanical behavior to old tissue when strained rapidly, despite not having the same underlying cellular architecture, and this, in turn, can help the whole frond survive high strain rates and rapid onsets of large hydrodynamic forces, such as those that may occur in impinging waves.

Old tissue in fronds of *E. menziesii* is already much stronger than the hydrodynamic forces it experiences in nature, so if a frond breaks from excessive hydrodynamic forces, it will likely break in the weak young tissue (Friedland and Denny, 1995; Burnett and Koehl, 2019). The strain-rate dependence of  $\sigma_{max}$ ,  $\sigma_{yield}$ , and  $W/V$  in the young tissue of fronds can benefit the entire kelp because it minimizes the risk that the young tissue will break when rapidly subjected to hydrodynamic forces. Breakage of *E. menziesii* fronds

removes their intercalary meristems and prevents further frond growth (i.e., elongation), although new fronds can grow out of the remaining frond tissue (Black, 1974). Breakage of numerous fronds on a single kelp can reduce its growth rate and long-term survival (Burnett and Koehl, 2020), so the strain-rate dependence of  $\sigma_{max}$ ,  $\sigma_{yield}$ , and  $W/V$  in only a few vulnerable regions of frond tissue can benefit the entire organism's performance. Strain-rate dependent material properties that enhance the mechanical behavior of young tissue may be more pronounced in macroalgal species where the majority of thallus tissue is grown from a basal meristem (i.e., young tissue is near the holdfast, old tissue is near the alga's distal tip) so that mechanical stresses are larger in young, proximal tissue than in old, distal tissue (Krumhansl et al., 2015).

The mechanical work required to break a kelp depends in part on the toughness of its tissues. Kelp tissue can be tough (i.e., have a high  $W/V$ ) by being strong (i.e., having a high  $\sigma_{max}$ ) and/or by being extensible (i.e., having a high  $\lambda_{max}$ ), and tissues that yield before breaking can be tough by absorbing mechanical energy by plastic deformation (e.g., Koehl, 1982, 1984; Janot and Martone, 2016). The  $\sigma_{max}$ ,  $\sigma_{yield}$ , and  $W/V$  (but not  $\lambda_{max}$ ) of the rachis tissue in *E. menziesii* tends to increase with tissue age, suggesting that tissue strength contributes more than extensibility to the age-related increase in toughness. Rachis tissue of *E. menziesii* at all ages is highly extensible. Having a high  $\lambda_{max}$  can allow the rachis to deform and absorb mechanical energy during brief pulses of rapid water motion. If the pulse of high load is very brief, as during wave impingement, then the extensible rachis tissue may not be stretched far enough to reach its breaking stress, as observed in the kelp *Nereocystis luetkeana* (Koehl and Wainwright, 1977). Thus, although strength and toughness of rachis tissue increase with age, the high extensibility of the rachis at all ages helps protect it from breakage during brief pulses of rapid water motion.

Here, we showed that the material properties of *E. menziesii* rachis tissue are not static traits but instead depend on the rate at which they are strained. We also showed that these strain-rate dependencies change with the tissue's age. Young rachis tissue (i.e., near the meristem) displayed increased strength, resistance to plastic deformation, and toughness when strained rapidly (simulating wave impingement) than when strained slowly (simulating wave surge), whereas old rachis tissue (i.e., far from the meristem) did not show the same effects of strain rate. Young rachis tissue is typically the weakest tissue on a frond, and breakage of the young tissue, which is coupled with the loss of the frond's meristem, can reduce a kelp's growth and survival. Therefore, we conclude that the entire kelp benefits from having strain-rate dependencies in the young, weak tissue of fronds that enhance that tissue's mechanical resistance to breakage during the rapid onset of hydrodynamic forces and strains, such as those that occur in crashing waves.

## ACKNOWLEDGMENTS

The authors thank two anonymous reviewers for their constructive feedback that greatly improved the manuscript.

## FUNDING INFORMATION

This work was funded by a Point Reyes National Seashore Marine Science Fund grant and the National Science Foundation

(DGE-1106400 to N.P.B.; DGE-0903711 to R. Full, M.A.R.K., R. Dudley, and R. Fearing).

## AUTHOR CONTRIBUTIONS

N.P.B. was responsible for data curation, formal analysis, investigation (carrying out field- and lab work), validation, and writing the original draft. M.A.R.K. was responsible for supervision. Both authors were responsible for conceptualization, funding acquisition, methodology, project administration, visualization, and reviewing and editing the final manuscript.

## DATA AVAILABILITY

Data are available from the Dryad Digital Repository at <https://doi.org/10.25338/B87914> (Burnett and Koehl, 2021).

## LITERATURE CITED

- Abbott, I. A., and G. J. Hollenberg. 1976. Marine algae of California. Stanford University Press, Stanford, CA, USA.
- Alexander, R. M. 1964. Visco-elastic properties of the mesogloea of jellyfish. *Journal of Experimental Biology* 41: 363–369.
- Armstrong, S. L. 1988. Mechanical properties of the tissues of the brown alga *Hedophyllum sessile* (C. Ag.) Setchell: variability with habitat. *Journal of Experimental Marine Biology and Ecology* 114: 143–151.
- Black, R. 1974. Some biological interactions affecting intertidal populations of the kelp *Egregia laevigata*. *Marine Biology* 28: 189–198.
- Biedka, R. F., J. M. Gosline, and R. E. DeWreede. 1987. Biomechanical analysis of wave-induced mortality in the marine alga *Pterygophora californica*. *Marine Ecology Progress Series* 36: 163–170.
- Burnett, N. P., and M. A. R. Koehl. 2018. Knots and tangles weaken kelp fronds while increasing drag forces and epifauna on the kelp. *Journal of Experimental Marine Biology and Ecology* 508: 13–20.
- Burnett, N. P., and M. A. R. Koehl. 2019. Mechanical properties of the wave-swept kelp *Egregia menziesii* change with season, growth rate and herbivore wounds. *Journal of Experimental Biology* 222: jeb190595.
- Burnett, N. P., and M. A. R. Koehl. 2020. Thallus pruning does not enhance survival or growth of a wave-swept kelp. *Marine Biology* 167: 52.
- Burnett, N. P., and M. A. R. Koehl. 2021. Data from: Age affects the strain-rate dependence of mechanical properties of kelp tissues. *Dryad Data Repository* <https://doi.org/10.25338/B87914>.
- Carrington, E. 1990. Drag and dislodgment of an intertidal macroalga: consequences of morphological variation in *Mastocarpus papillatus* Kützing. *Journal of Experimental Marine Biology and Ecology* 139: 185–200.
- Carrington, E., and J. M. Gosline. 2004. Mechanical design of mussel byssus: load cycle and strain rate dependence. *American Malacological Bulletin* 18: 135–140.
- Delf, E. M. 1932. Experiments with the stipes of *Fucus* and *Laminaria*. *Journal of Experimental Biology* 9: 300–313.
- Demes, K. W., J. N. Pruitt, C. D. Harley, and E. Carrington. 2013. Survival of the weakest: increased frond mechanical strength in a wave-swept kelp inhibits self-pruning and increases whole-plant mortality. *Functional Ecology* 27: 439–445.
- Denny, M. W. 1988. Biology and the mechanics of the wave-swept environment. Princeton University Press, Princeton, NJ, USA.
- Denny, M. W., and J. M. Gosline. 1980. The physical properties of the pedal mucus of the terrestrial slug, *Ariolimax columbianus*. *Journal of Experimental Biology* 88: 375–393.
- Denny, M. W., K. Mach, S. Tepler, and P. Martone. 2013. Indefatigable: an erect coralline alga is highly resistant to fatigue. *Journal of Experimental Biology* 216: 3772–3780.
- Derby, B., and R. Akhtar [eds.]. 2015. Mechanical properties of aging soft tissues. Springer International, Cham, Switzerland.
- Friedland, M. T., and M. W. Denny. 1995. Surviving hydrodynamic forces in a wave-swept environment: consequences of morphology in the feather boa kelp, *Egregia menziesii* (Turner). *Journal of Experimental Marine Biology and Ecology* 190: 109–133.
- Gaylord, B. 1999. Detailing agents of physical disturbance: wave-induced velocities and accelerations on a rocky shore. *Journal of Experimental Marine Biology and Ecology* 239: 85–124.
- Gaylord, B., M. W. Denny, and M. A. R. Koehl. 2003. Modulation of wave forces on kelp canopies by alongshore currents. *Limnology and Oceanography* 48: 860–871.
- Gaylord, B., M. W. Denny, and M. A. R. Koehl. 2008. Flow forces on seaweeds: field evidence for roles of wave impingement and organism inertia. *Biological Bulletin* 215: 295–308.
- Hale, B. 2001. Macroalgal materials: foiling fracture and fatigue from fluid forces. Ph.D. dissertation, Stanford University, Stanford, CA, USA.
- Harder, D. L., C. L. Hurd, and T. Speck. 2006. Comparison of mechanical properties of four large, wave-exposed seaweeds. *American Journal of Botany* 93: 1426–1432.
- Hayot, C. M., E. Forouzesh, G. Ashwani, Z. Avramova, and J. A. Turner. 2012. Viscoelastic properties of cell walls of single living plant cells determined by dynamic nanoindentation. *Journal of Experimental Botany* 63: 2525–2540.
- Henry, P.-Y. 2018. Variability and similarities in the structural properties of two related *Laminaria* kelp species. *Estuarine, Coastal and Shelf Science* 200: 395–405.
- Janot, K., and P. T. Martone. 2016. Convergence of joint mechanics in independently evolving articulated coralline algae. *Journal of Experimental Biology* 219: 383–391.
- Jensen, M. M., and M. W. Denny. 2015. Experimental determination of the hydrodynamic forces responsible for wave impact events. *Journal of Experimental Marine Biology and Ecology* 469: 123–130.
- Johnson, A. S., and M. A. R. Koehl. 1994. Maintenance of dynamic strain similarity and environmental stress factor in different flow habitats: thallus allometry and material properties of a giant kelp. *Journal of Experimental Biology* 195: 381–410.
- Kitzes, J. A., and M. W. Denny. 2005. Red algae respond to waves: morphological and mechanical variation in *Mastocarpus papillatus* along a gradient of force. *Biological Bulletin* 208: 114–119.
- Koehl, M. A. R. 1977. Mechanical diversity of the connective tissue of the body wall of sea anemones. *Journal of Experimental Biology* 69: 107–125.
- Koehl, M. A. R. 1982. The interaction of moving water and sessile organisms. *Scientific American* 247: 124–132.
- Koehl, M. A. R. 1984. How do benthic organisms withstand moving water? *American Zoologist* 24: 57–70.
- Koehl, M. A. R. 1986. Seaweeds in moving water: form and function. In T. J. Givnish [ed.], *On the economy of plant form and function*, 603–634. Cambridge University Press, Cambridge, UK.
- Koehl, M. A. R. 1999. Ecological biomechanics: life history, mechanical design, and temporal patterns of mechanical stress. *Journal of Experimental Biology* 202: 3469–3476.
- Koehl, M. A. R. 2000. Mechanical design and hydrodynamics of blade-like algae: *Chondracanthus exasperatus*. In H. C. Spatz, and T. Speck [eds.], *Proceedings of the Third International Conference on Plant Biomechanics*, 295–308. Thieme Verlag, Stuttgart, Germany.
- Koehl, M. A. R., and R. S. Alberte. 1988. Flow, flapping, and photosynthesis of macroalgae: functional consequences of undulate blade morphology. *Marine Biology* 99: 435–444.
- Koehl, M. A. R., and S. A. Wainwright. 1977. Mechanical adaptations of a giant kelp. *Limnology and Oceanography* 22: 1067–1071.
- Koehl, M. A. R., and S. A. Wainwright. 1985. Biomechanics. In M. L. Littler and D. S. Littler [eds.], *Handbook of phycological methods. Ecological field methods: Macroalgae*, 292–313. Cambridge University Press, Cambridge, UK.
- Krumhansl, K. A., K. W. Demes, E. Carrington, and C. D. G. Harley. 2015. Divergent growth strategies between red algae and kelps influence biomechanical properties. *American Journal of Botany* 102: 1938–1944.

- Lowell, R. B., J. H. Markham, and K. H. Mann. 1991. Herbivore-like damage induces increased strength and toughness in a seaweed. *Proceedings of the Royal Society of London, B, Biological Sciences* 243: 31–38.
- Mach, K. J. 2009. Mechanical and biological consequences of repetitive loading: crack initiation and fatigue failure in the red macroalga *Mazzaella*. *Journal of Experimental Biology* 212: 961–976.
- Mason, T. G., and D. A. Weitz. 1995. Optical measurements of frequency-dependent linear viscoelastic moduli of complex fluids. *Physical Review Letters* 74: 1250–1253.
- Meinzer, F. C., B. Lachenbruch, and T. E. Dawson [eds.]. 2011. Size- and age-related changes in tree structure and function. Springer, Dordrecht, Netherlands.
- Meyers, M. A., and P.-Y. Chen. 2014. Biological materials science. Cambridge University Press, Cambridge, UK.
- Morgan, E. F., G. U. Unnikrisnan, and A. I. Hussein. 2018. Bone mechanical properties in healthy and diseased states. *Annual Review of Biomedical Engineering* 20: 119–143.
- O'Donnell, M. J., and M. W. Denny. 2008. Hydrodynamic forces and surface topography: centimeter-scale spatial variation in wave forces. *Limnology and Oceanography* 53: 579–588.
- R Core Team. 2020. R: a language and environment for statistical computing. R Foundation for Statistical Computing, Vienna, Austria. Website: <https://www.R-project.org/>.
- Sahni, V., T. A. Blackledge, and A. Dhinojwala. 2010. Viscoelastic solids explain spider web stickiness. *Nature Communications* 1: 19.
- Starko, S., S. D. Mansfield, and P. T. Martone. 2018. Cell wall chemistry and tissue structure underlie shifts in material properties of a perennial kelp. *European Journal of Phycology* 53: 307–317.
- Stewart, H. L. 2006. Ontogenetic changes in tissue strength, buoyancy and reproductive investment in the tropical rafting macroalga *Turbinaria ornata*. *Journal of Phycology* 42: 43–50.
- Vettori, D., and V. Nikora. 2017. Morphological and mechanical properties of blades of *Saccharina latissimi*. *Estuarine, Coastal and Shelf Science* 196: 1–9.
- Vincent, J. V. 2012. Structural biomaterials. Princeton University Press, Princeton, NJ, USA.
- Wolcott, B. D. 2007. Mechanical size limitation and life-history strategy of an intertidal seaweed. *Marine Ecology Progress Series* 338: 1–10.
- Zhou, T., J. Yan, J. Masuda, and T. Kuriyagawa. 2009. Investigation on the viscoelasticity of optical glass in ultraprecision lens molding process. *Journal of Materials Processing Technology* 209: 4484–4489.